

## Supporting Information

# Biaxial negative thermal expansion in $\text{Zn}[\text{N}(\text{CN})_2]_2$

Ya Zhang,<sup>a</sup> Andrea Sanson,<sup>b</sup> Yuzhu Song,<sup>a</sup> Luca Olivi,<sup>c</sup> Naïke Shi,<sup>\*a</sup> Lei Wang<sup>\*d</sup> and Jun Chen<sup>a</sup>

<sup>a</sup> Beijing Advanced Innovation Center for Materials Genome Engineering, Department of Physical Chemistry, University of Science and Technology Beijing, Beijing 100083, China

<sup>b</sup> Department of Physics and Astronomy, University of Padova, Padova I-35131, Italy

<sup>c</sup> Department of Elettra Sincrotrone Trieste, I-34149 Basovizza, Italy

<sup>d</sup> Department of Physics, University of Science and Technology Beijing, Beijing 100083, China

E-mail address: [naike@ustb.edu.cn](mailto:naike@ustb.edu.cn) (N. Shi), [leiw\\_phy@ustb.edu.cn](mailto:leiw_phy@ustb.edu.cn) (L. Wang).

## List of Contents

### Experimental section

**Fig. S1.** TG-DSC curve of  $\text{Zn}[\text{N}(\text{CN})_2]_2$ .

**Fig. S2.** SEM image of  $\text{Zn}[\text{N}(\text{CN})_2]_2$  sample.

**Fig. S3.** High-temperature XRD patterns of  $\text{Zn}[\text{N}(\text{CN})_2]_2$ .

**Fig. S4.** Best-fitting high-resolution XRD at 300 K of  $\text{Zn}[\text{N}(\text{CN})_2]_2$ .

**Fig. S5.** A cyclic thermal expansion test (Temperature from 173K to 473K to 173K) of  $\text{Zn}[\text{N}(\text{CN})_2]_2$ .

**Fig. S6.** The  $\text{ZnN}_4$  polyhedra volume, which fluctuates around  $4.7\text{\AA}^3$ .

**Fig. S7.**  $k^2$ -weighted Zn EXAFS signals collected in  $\text{Zn}[\text{N}(\text{CN})_2]_2$  as a function of temperature (left panel) and corresponding Fourier Transform (right panel), here performed with  $k=2.5-14\text{\AA}^{-1}$ ,  $k^2$ , Gaussian window.

**Fig. S8.** Modulus and imaginary part of the Fourier transform of the EXAFS.

**Fig. S9.** Bond thermal expansions obtained by EXAFS in  $\text{Zn}[\text{N}(\text{CN})_2]_2$  and parallel MSRDS.

**Fig. S10.** Linear fit of the average Zn-N and Zn-C bond thermal expansion measured by XRD.

**Fig. S11.** Raman mode frequency shifts as a function of pressure for



**Table S1.** Scattering paths related to the FT structure between about 0.8 and 3.3 Å calculated by FEFF code<sup>1</sup>. The last column lists the used fitting parameters (distance, Debye-Waller factor, third and fourth cumulant) reduced as much possible to stabilize the fitting analysis.

**Table S2.** Calculated bond stretching and bond bending effective force constants and anisotropy.

## Experimental section

### Materials

Reagents used in synthesis: Na[N(CN)<sub>2</sub>] (97%, Shanghai Shaoyuan Reagent Ltd), Zn(NO<sub>3</sub>)<sub>2</sub>•6H<sub>2</sub>O (99.0%, Sinopharm Chemical Reagent Ltd).

### Preparation of Zn[N(CN)<sub>2</sub>]<sub>2</sub>

The synthesis of Zn[N(CN)<sub>2</sub>]<sub>2</sub> is via simple solution precipitation method. 0.2204 g (2.48 mmol) of Na[N(CN)<sub>2</sub>] were placed in a 50 mL beaker and dissolved in 10 mL of deionized water with stirring. In a 10 mL beaker, 0.3689 g (1.24 mmol) of Zn(NO<sub>3</sub>)<sub>2</sub>•6H<sub>2</sub>O were dissolved in 5 mL of deionized water. Then the two colorless solutions were mixed, and a white precipitate was formed immediately. The mixture was stirred for four hours in an open beaker. The product was then filtered off, washed with alcohol to remove ionic impurity. The dried yield was about 0.2188 g.

### Characterization

Room temperature and variable temperature X-ray diffraction (XRD) data were collected by PANalytical, PW3040-X 'Pert Pro X-ray diffractometer (Cu, K $\alpha$ , 40kV, 40mA). The XRD patterns were refined by Fullprof software based on Rietveld analysis method.

Thermogravimetric - differential scanning calorimetry (TG-DSC) measurement was carried out using Mettler-Toledo instruments at the heating rate of 5K min<sup>-1</sup> from 323K to 1173K. Approximately 15 mg samples were loaded into a crucible and the measurement results are recorded in oxygen and nitrogen atmosphere.

The microstructure information of the sample was conducted on Carl Zeiss field emission scanning electron microscope (FE-SEM,SURA-40).

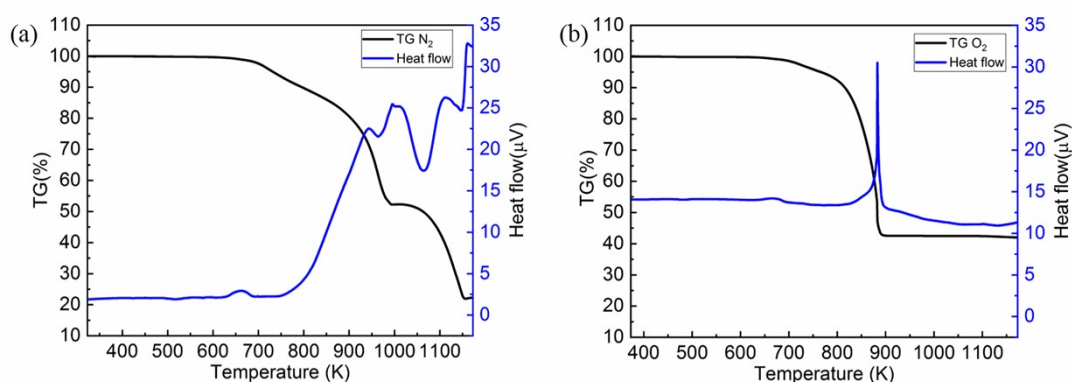
Zn K-edge EXAFS measurements were performed in  $\text{Zn}[\text{N}(\text{CN})_2]_2$  from 100 K to 340 K with step of 40 K at the XAFS beamline of ELETTRA synchrotron facility in Trieste (Italy). The samples for EXAFS were prepared by mixing and pelletizing the samples powder with boron nitride powder, and the amount of sample powder was chosen to have an absorption edge jump  $\Delta\mu_x \sim 1$ . The EXAFS spectra were collected in transmission mode in the energy range  $\sim 9.4$ - $10.9$  keV for Zn, with an energy step varying from 0.2 eV in the near-edge region to about  $\sim 4$  eV at the highest energies, thus to obtain a uniform wave vector step  $\Delta k \sim 0.03 \text{ \AA}^{-1}$ . The x-ray beam was monochromatized by a Si(111) double-crystal monochromator. The sample was kept under high-vacuum ( $< 10^{-5}$  mbar) during the entire experiment, was mounted in a helium cryostat combined with an electric heater and the temperature was stabilized and controlled by a feedback loop, ensuring a thermal stability within  $\pm 1$  K. At least two spectra were collected at each temperature point.

EXAFS data analysis was performed according to well established procedures by using FEFF<sup>1</sup> and FEFFIT<sup>2</sup> codes. The  $k^2$ -weighted EXAFS signals and the corresponding Fourier Transforms are shown in Fig. S7. The scattering contributions related to the first two FT peaks are reported in Table S1. A non-linear best fit of the experimental spectra was then performed in the  $r$ -space between about 0.8 and 3.3  $\text{\AA}$  (examples shown in Fig. S8). The finale results were obtained as average on different FTs ( $k_{\text{min}} = 2 \div 3 \text{ \AA}^{-1}$  and  $k_{\text{max}} = 12 \div 15 \text{ \AA}^{-1}$ ,  $k$ -weight = 1 and 2) and fitting range (from

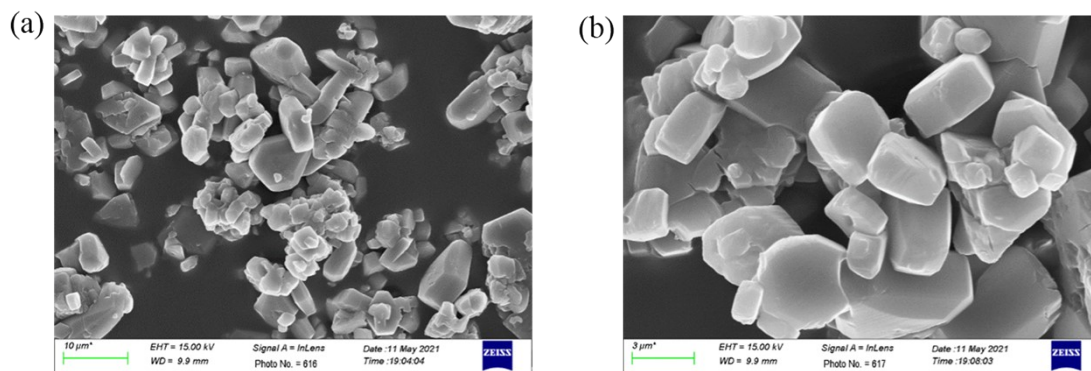
$r=0.8-1.0$  to  $3.1-3.3 \text{ \AA}$ ).

Fig. S9 shows the temperature dependence of the first and second EXAFS cumulants obtained for the Zn-N, Zn-C and C-N bond distances. Table S2 reports the bond stretching and bond bending effective force constants and anisotropy estimated through the best-fitting Einstein models. This is an approximate estimation because affected by the linear fit of XRD results reported in Fig. S10.

The variable temperature Raman spectra were subjected by HR Evolution, Horiba Raman spectrometer ( $\lambda = 532\text{nm}$ ,  $148\text{K}-448\text{K}$ ). The variable voltage Raman scattering was performed on Horiba Jobin Yvon Labram HR evolution spectrometer and semiconductor cooled CCD detector under confocal backscattering geometry ( $\lambda = 532\text{nm}$   $0-3.94\text{GPa}$ ). The spectrometer is equipped with  $1800\text{g mm}^{-1}$  grating option. In the high pressure Raman experiment, the sample was stored in a diamond anvil containing a small amount of ruby for pressure calibration, and the pressure transfer medium was silicone oil.



**Fig. S1.** TG-DSC curve of  $\text{Zn}[\text{N}(\text{CN})_2]_2$ . (a).  $\text{N}_2$  atmosphere,  $5\text{K}/\text{min}$  heating rate, (b).  $\text{O}_2$  atmosphere,  $5\text{K}/\text{min}$  heating rate.



**Fig. S2.** SEM image of  $\text{Zn}[\text{N}(\text{CN})_2]_2$  sample.

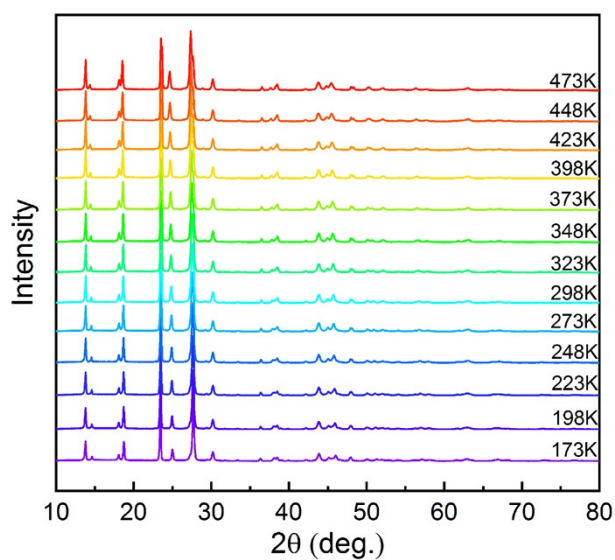


**Fig. S3.** High-temperature XRD patterns of  $\text{Zn}[\text{N}(\text{CN})_2]_2$

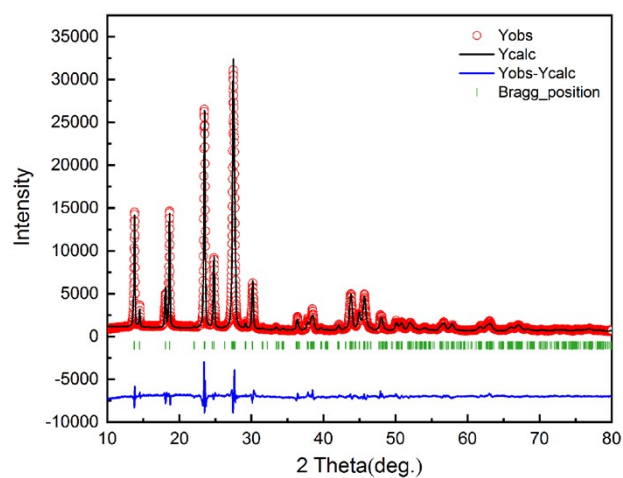


**Fig. S4.** Best-fitting high-resolution XRD at 300 K of  $\text{Zn}[\text{N}(\text{CN})_2]_2$

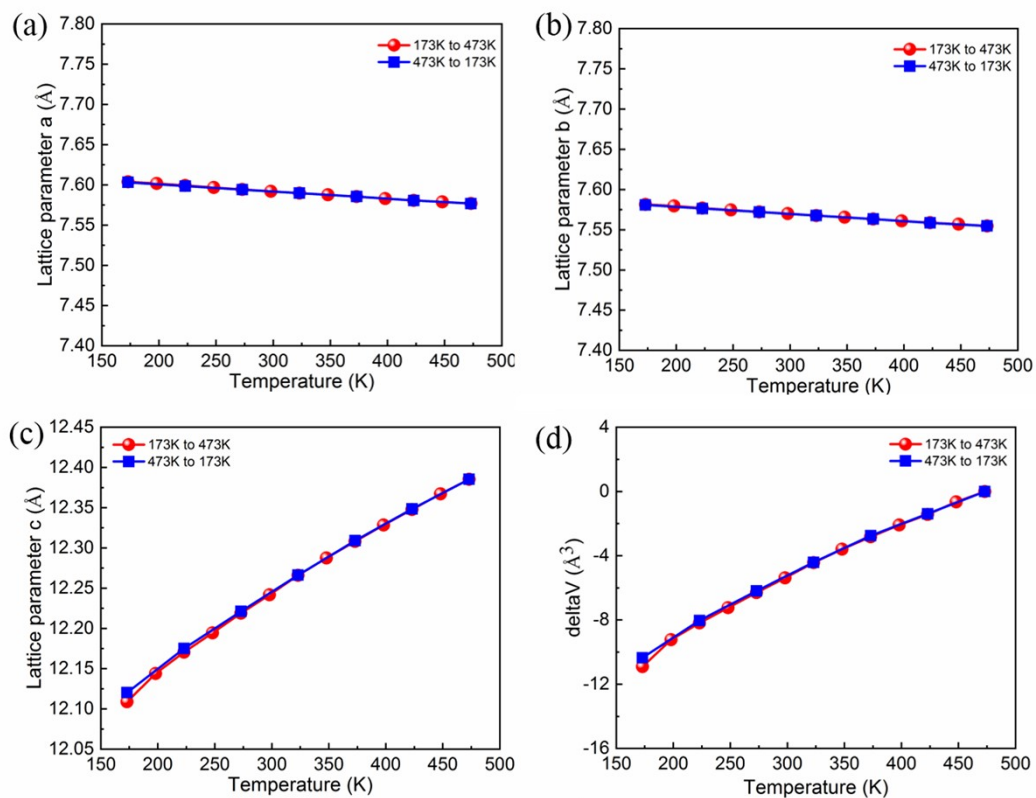


**Fig. S5.** A cyclic thermal expansion test (Temperature from 173K to 473K to 173K) of Zn[N(CN)<sub>2</sub>]<sub>2</sub>.

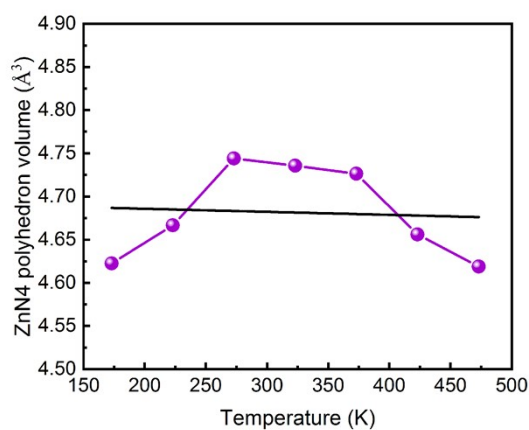


**Fig. S6.** The ZnN<sub>4</sub> polyhedra volume, which fluctuates around 4.7 Å<sup>3</sup>.



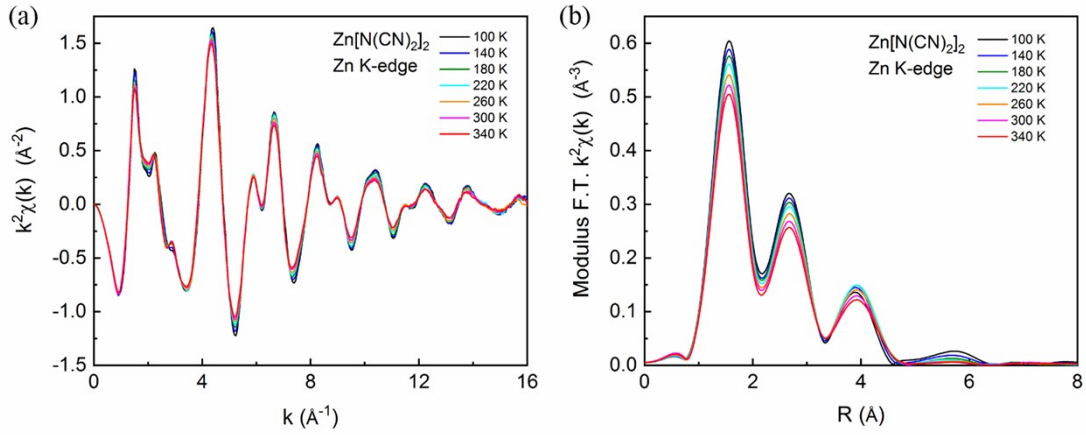


**Fig. S7.**  $k^2$ -weighted Zn EXAFS signals collected in  $\text{Zn}[\text{N}(\text{CN})_2]_2$  as a function of temperature (left panel) and corresponding Fourier Transform (right panel), here performed with  $k=2.5\text{-}14 \text{ \AA}^{-1}$ ,  $k^2$ , Gaussian window.

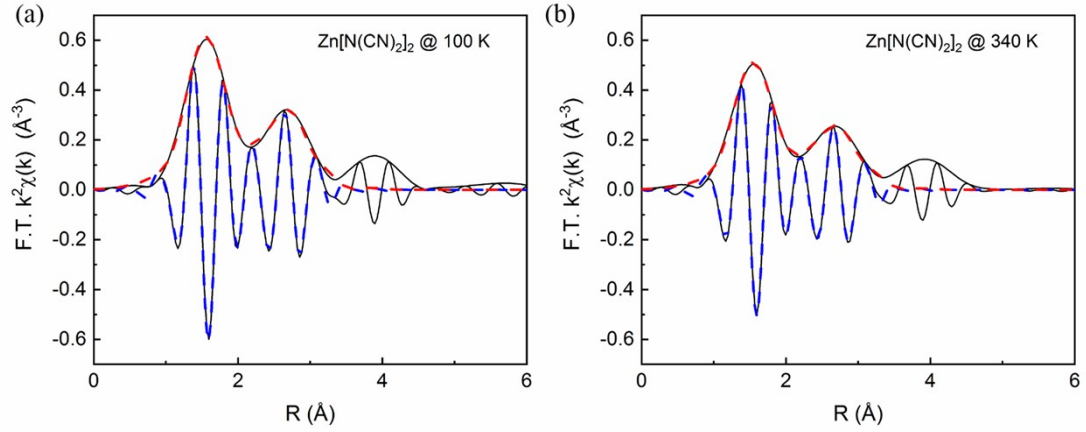


**Fig. S8.** Modulus and imaginary part of the Fourier transform of the EXAFS signal (continuous lines) and best-fitting simulation (dashed-bold lines) at 100 K and 340 K (left and right panel, respectively).

**Table S1.**

Scattering paths related to the FT structure between about 0.8 and 3.3  $\text{\AA}$  calculated by FEFF code [1]. The last column lists the used fitting parameters (distance, Debye-Waller factor, third and fourth cumulant) reduced as much possible to stabilize the fitting analysis.

Index	Path	Legs	Degeneracy	reff ( $\text{\AA}$ )	Amplitude	Parameters
1	Zn-N	2	1	1.9392	100.00	$r_N, \sigma_N^2, C_{3N}, C_{4N}$
2	Zn-N	2	2	2.1064	164.82	
3	Zn-N	2	1	2.1884	75.34	
4	Zn-C	2	1	3.1370	27.74	$r_C, \sigma_C^2, C_{3C}, C_{4C}$
7	Zn-C	2	3	3.2031	78.99	

5	Zn-N-C	3	2	3.1422	100.81	$r_N, \sigma_N^2, r_C, \sigma_C^2,$ $r_{CN}, \sigma_{CN}^2$
6	Zn-N-C-N	4	1	3.1474	94.84	$r_N, \sigma_N^2,$ $r_{CN}, \sigma_{CN}^2$
8	Zn-N-C	3	2	3.2038	107.51	$r_N, \sigma_N^2, r_C, \sigma_C^2,$ $r_{CN}, \sigma_{CN}^2$
9	Zn-N-C-N	4	1	3.2038	114.99	$r_N, \sigma_N^2,$ $r_{CN}, \sigma_{CN}^2$
10	Zn-N-C	3	4	3.2749	121.76	$r_N, \sigma_N^2, r_C, \sigma_C^2,$ $r_{CN}, \sigma_{CN}^2$

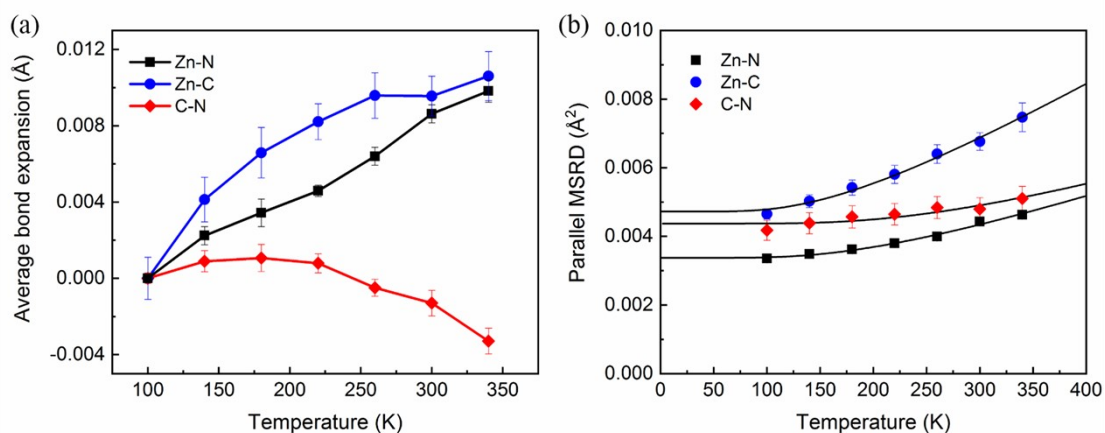


**Fig. S9.** Bond thermal expansions obtained by EXAFS in Zn[N(CN)<sub>2</sub>]<sub>2</sub> (left panel) and parallel MSRDS (right panel). Solid lines in the right panel correspond to the best-fitting Einstein model whose results are reported in the column “stretching” of Table S2.

**Table S2.**

Calculated bond stretching and bond bending effective force constants and anisotropy.

	Stretching	Bending	Anisotropy
Zn-N	$12.98 \pm 0.20$ THz	$6.39 \pm 0.26$ THz	$\gamma = 2k_{\parallel}/k_{\perp} = 7 \pm 1$

	$k_{\parallel} = 7.95 \pm 0.24 \text{ eV/\AA}^2$	$k_{\perp} = 1.93 \pm 0.16 \text{ eV/\AA}^2$	
<b>Zn-C</b>	$10.54 \pm 0.15 \text{ THz}$ $k_{\parallel} = 4.61 \pm 0.13 \text{ eV/\AA}^2$	$1.83 \pm 0.04 \text{ THz}$ $k_{\perp} = 0.14 \pm 0.01 \text{ eV/\AA}^2$	$\gamma = 2k_{\parallel}/k_{\perp} = 54 \pm 3$
<b>C-N</b>	$17.87 \pm 0.93 \text{ THz}$ $k_{\parallel} = 8.45 \pm 0.88 \text{ eV/\AA}^2$		

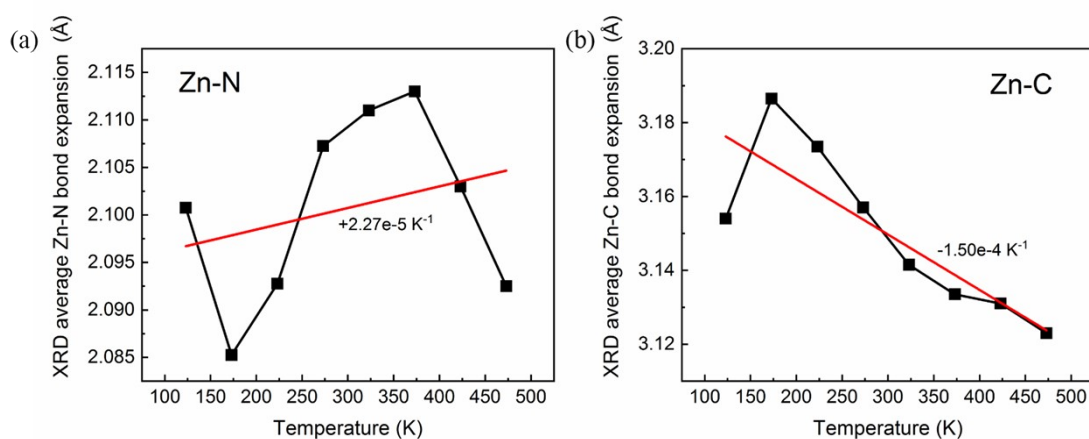


**Fig. S10.** Linear fit of the average Zn-N and Zn-C bond thermal expansion measured by XRD, then used to determined the perpendicular MSRDS.

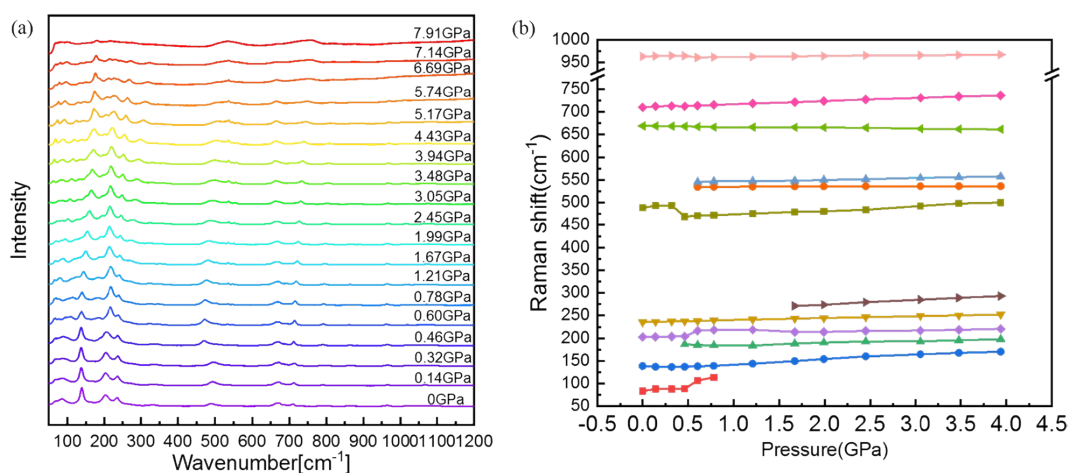


**Fig. S11.** Raman mode frequency shifts as a function of pressure for Zn[N(CN)<sub>2</sub>]<sub>2</sub>.

## References

1. M. Newville, B. Ravel, D. Haskel, J. Rehr, E. Stern and Y. Yacoby, Analysis of multiple-scattering XAFS data using theoretical standards, *Physica B: Condensed Matter*, 1995, **208**, 154-156.
2. A. L. Ankudinov, B. Ravel, J. Rehr and S. Conradson, Real-space multiple-scattering calculation and interpretation of x-ray-absorption near-edge structure, *Physical Review B*, 1998, **58**, 7565.